Autophagy and inflammasome molecular interplay and activation predict poor response to FLT3 inhibitors in FLT3-ITD acute myeloid leukemia

Brunno Gilberto Santos de Macedo1; https://orcid.org/0000-0003-2352-6905

Manuela Albuquerque de Melo1; https://orcid.org/0000-0002-8413-5396

Diego Antonio Pereira-Martins2; https://orcid.org/0000-0002-3302-4311

João Agostinho Machado-Neto3; https://orcid.org/0000-0002-2937-8109

Fabíola Traina1; https://orcid.org/0000-0003-4258-289X

1 Department of Medical Images, Hematology, and Oncology, Ribeirão Preto Medical School, University of São Paulo, Ribeirão Preto, São Paulo, Brazil.

2 Department of Experimental Hematology, University of Groningen, 9718 BG Groningen, The Netherlands.

3 Department of Pharmacology, Institute of Biomedical Sciences, University of São Paulo, São Paulo, Brazil.

Address: 3900 Bandeirantes Avenue, Ribeirão Preto, São Paulo, Brazil, Zip Code 14040-900

Corresponding author: Fabíola Traina (ftraina@fmrp.usp.br)

SUPPLEMENTARY MATERIAL

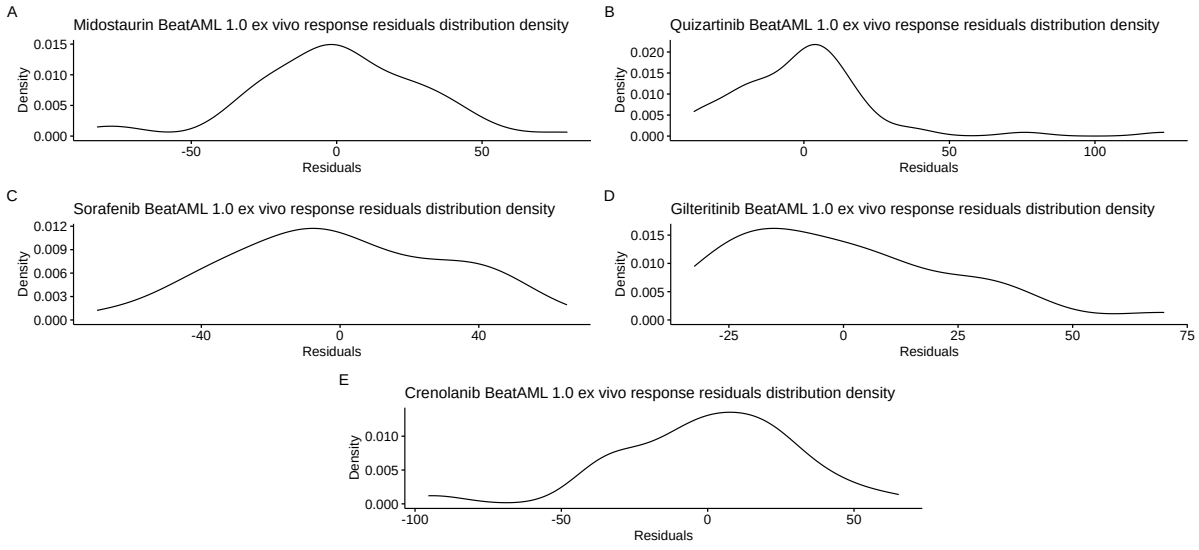

Figure S1. **Density plot as a graphical representation of the samples residuals from a linear regression distribution for (A) midostaurin, (B) quizartinib, (C) sorafenib, (D) gilteritinib, and (E) crenolanib.** Graphically representing the data aids the statistical characterization, in this case through a density plot, by displaying total data residual distribution.

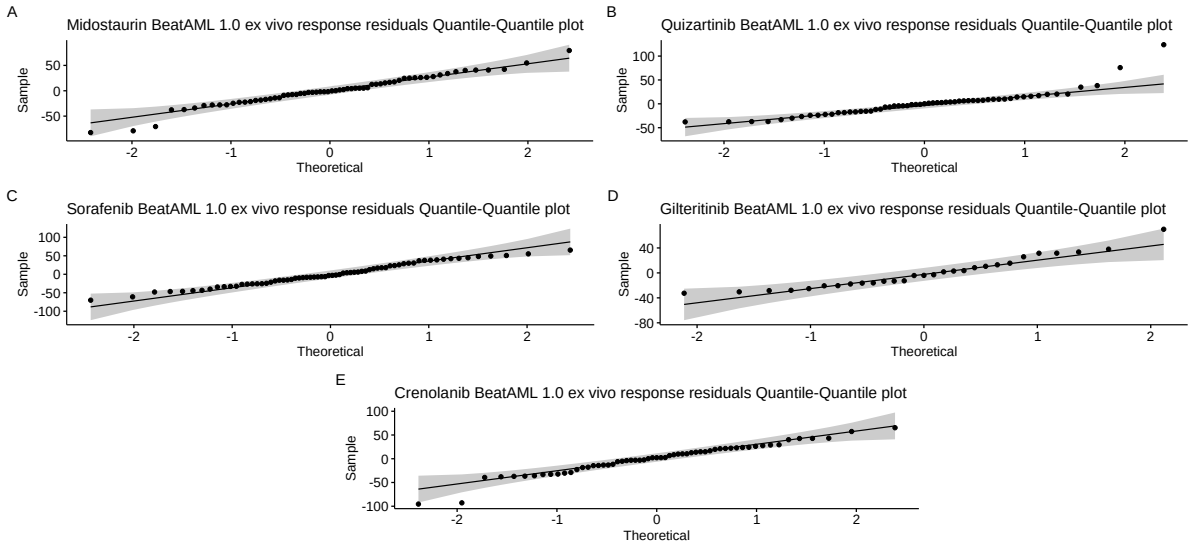

Figure S2. **Quantile-Quantile plot (Q-Q plot) as a graphical representation of correspondence between the samples residuals from a linear regression quantile and a theoretical normal distribution quantile for (A) midostaurin, (B) quizartinib, (C) sorafenib, (D) gilteritinib, and (E) crenolanib.** Graphically representing the data aids the statistical characterization, in this case through a Q-Q plot, by displaying total data residual distribution.

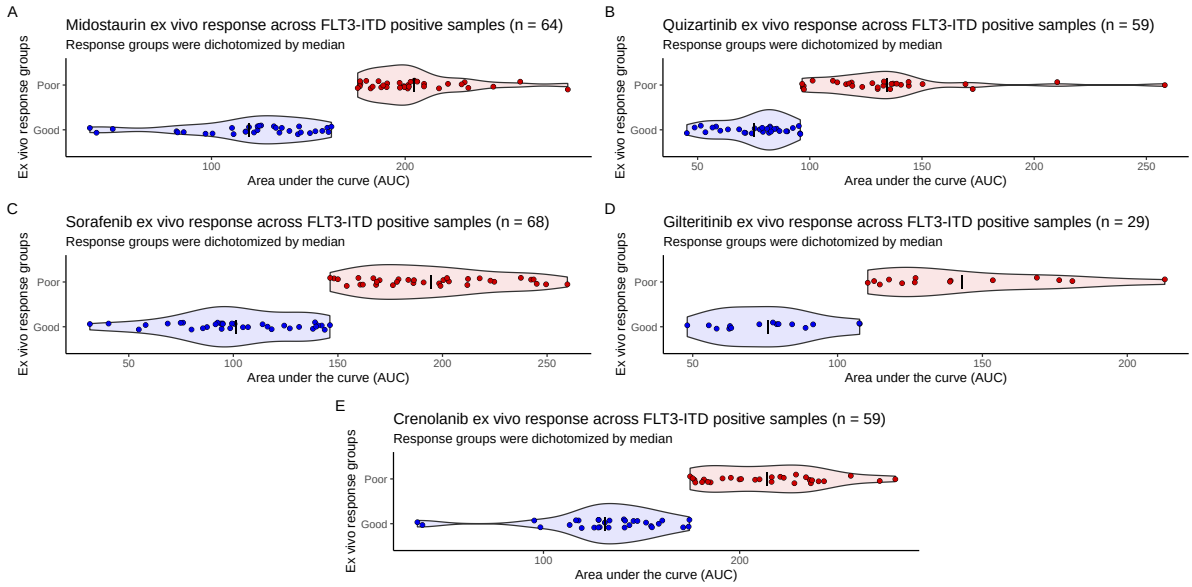

Figure S3. **Graphical representation of *ex vivo* drug response of (A) midostaurin, (B) quizartinib, (C) sorafenib, (D) gilteritinib, and (E) crenolanib measured in area under the curve (AUC).** Graphically representing the data aids the statistical characterization, in this case through a violin plot, by displaying grouped data distribution and their homogeneity.

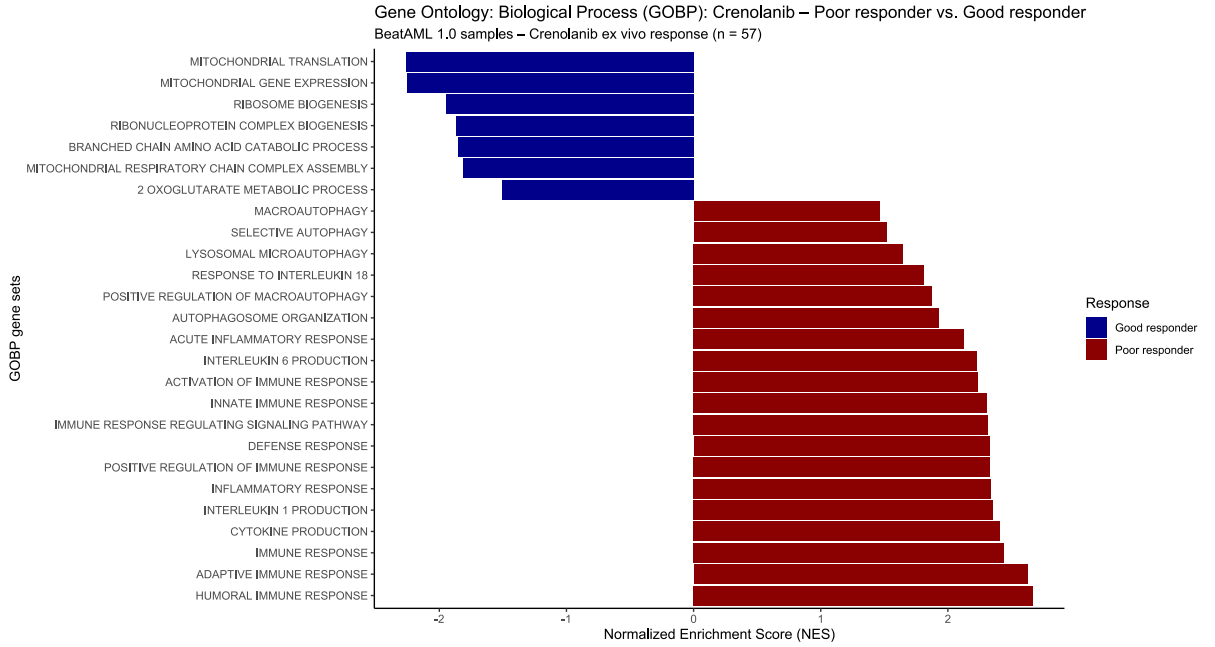

Figure S4. **Gene set enrichment analysis (GSEA) comparing *ex vivo* crenolanib response groups (57 samples).** The poor responders' group are represented by positively enriched gene sets (displayed on y-axis), since they are the reference group for comparison, while the negatively enriched gene sets are attributed to the good responders. This GSEA employs the gene sets comprised in the Gene Ontology: Biological Process (GOBP) human gene set collection.

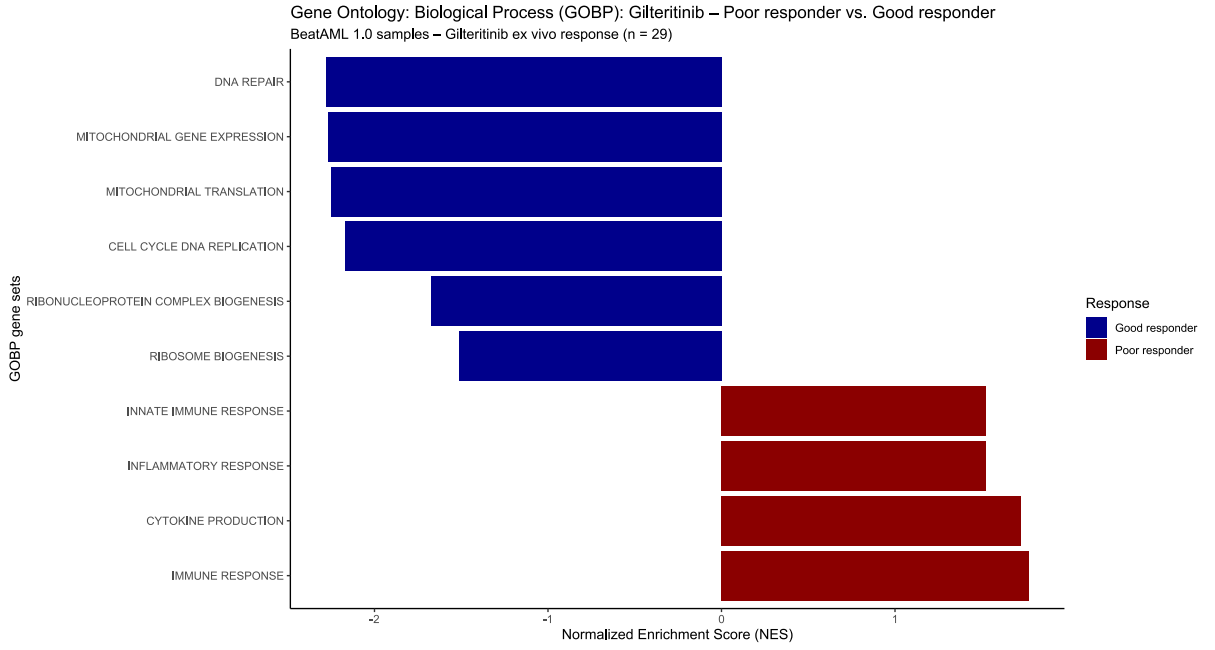

Figure S5. **Gene set enrichment analysis (GSEA) comparing *ex vivo* gilteritinib response groups (29 samples).** The poor responders' group are represented by positively enriched gene sets (displayed on y-axis), since they are the reference group for comparison, while the negatively enriched gene sets are attributed to the good responders. This GSEA employs the gene sets comprised in the Gene Ontology: Biological Process (GOBP) human gene set collection.

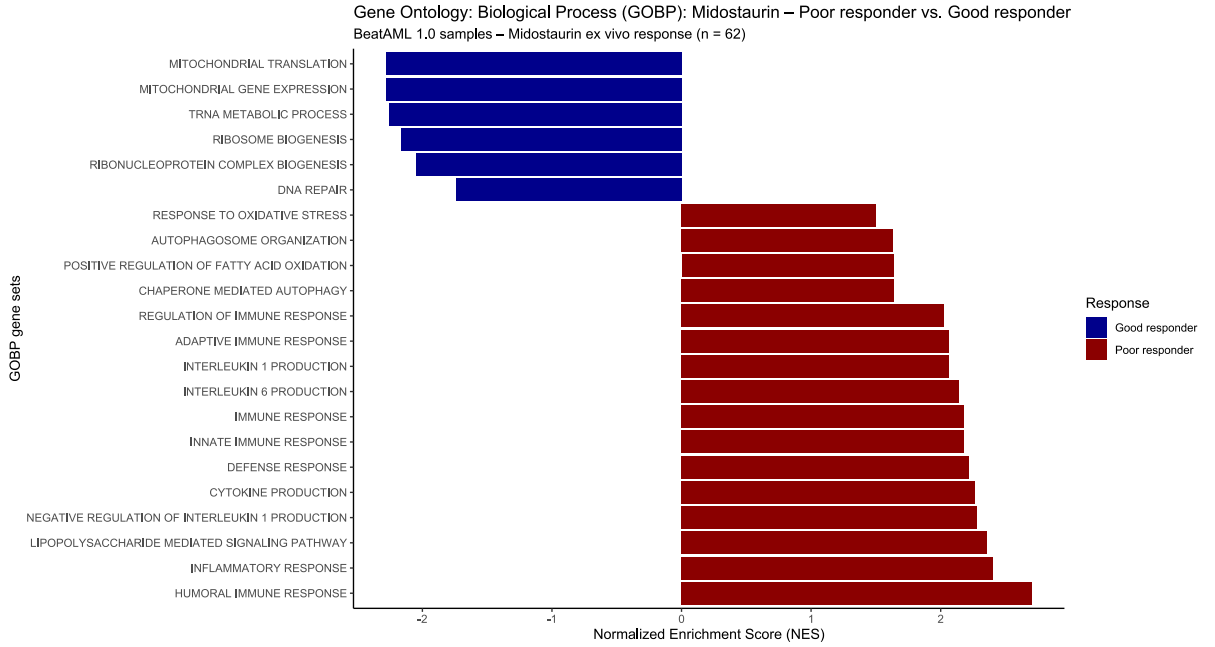

Figure S6. **Gene set enrichment analysis (GSEA) comparing *ex vivo* midostaurin response groups (62 samples).** The poor responders' group are represented by positively enriched gene sets (displayed on y-axis), since they are the reference group for comparison, while the negatively enriched gene sets are attributed to the good responders. This GSEA employs the gene sets comprised in the Gene Ontology: Biological Process (GOBP) human gene set collection.

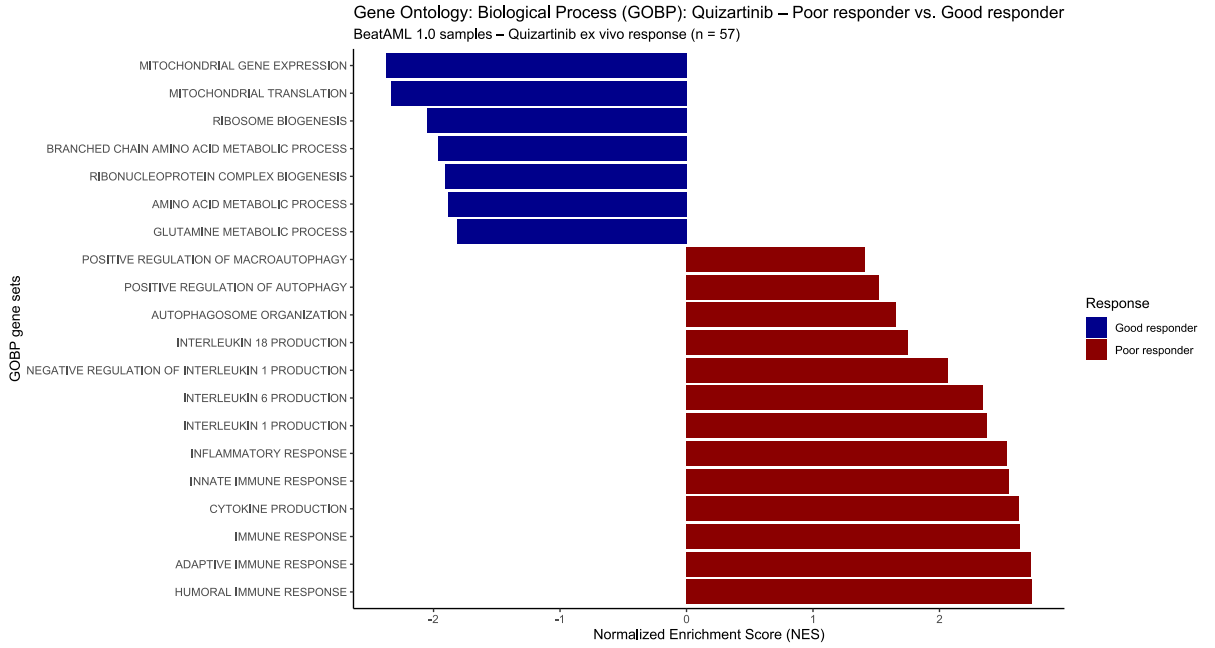

Figure S7. **Gene set enrichment analysis (GSEA) comparing *ex vivo* quizartinib response groups (57 samples).** The poor responders' group are represented by positively enriched gene sets (displayed on y-axis), since they are the reference group for comparison, while the negatively enriched gene sets are attributed to the good responders. This GSEA employs the gene sets comprised in the Gene Ontology: Biological Process (GOBP) human gene set collection.

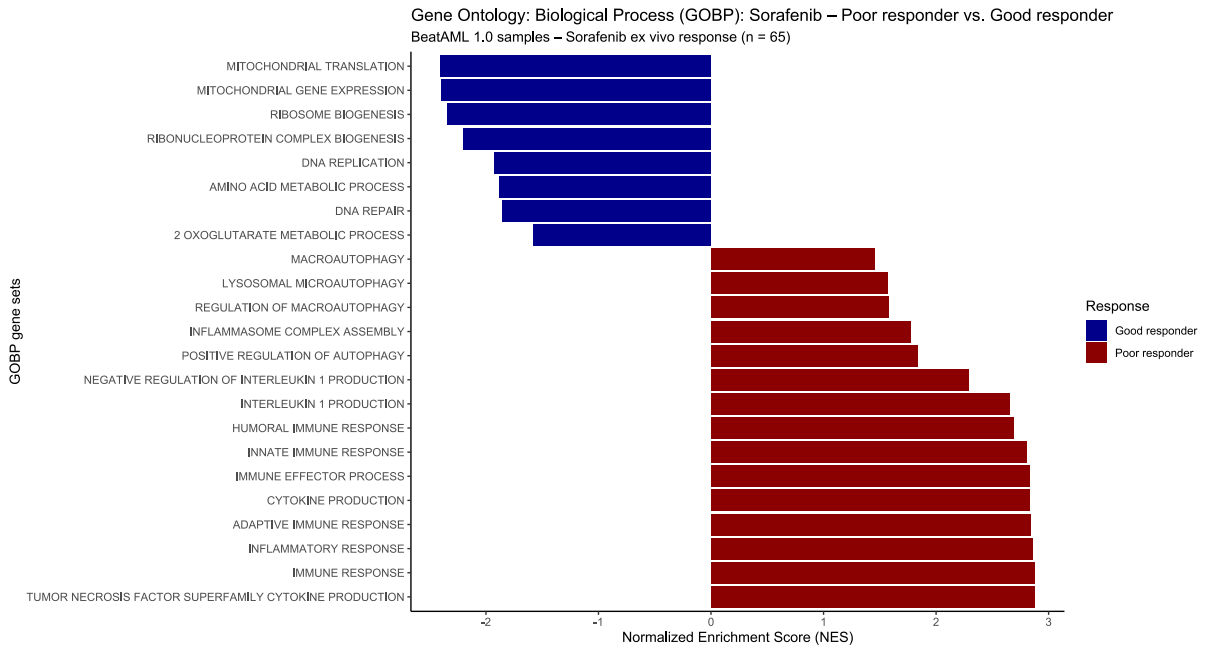

Figure S8. **Gene set enrichment analysis (GSEA) comparing *ex vivo* sorafenib response groups (65 samples).** The poor responders' group are represented by positively enriched gene sets (displayed on y-axis), since they are the reference group for comparison, while the negatively enriched gene sets are attributed to the good responders. This GSEA employs the gene sets comprised in the Gene Ontology: Biological Process (GOBP) human gene set collection.

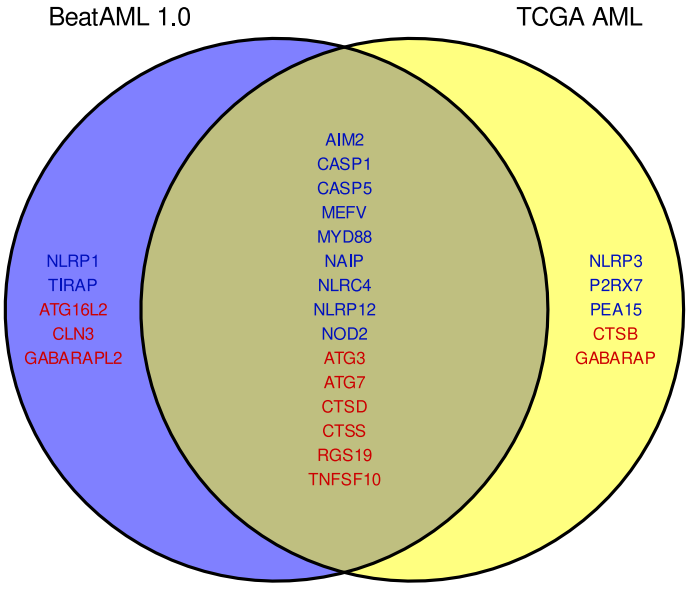

Figure S9. **Overlapped genes among the 20 strongest positive correlations between autophagy and inflammasome gene expression on adult AML patients from both databases (BeatAML 1.0 and TCGA AML).** In red, are the genes related to autophagy, in blue, related to inflammasome. Nine out of 15 (60%) correlated genes are inflammasome genes, whereas 6 out of 15 (40%) are autophagy genes. Fifteen out of 20 genes are common to both databases yielding a 75% correlation.

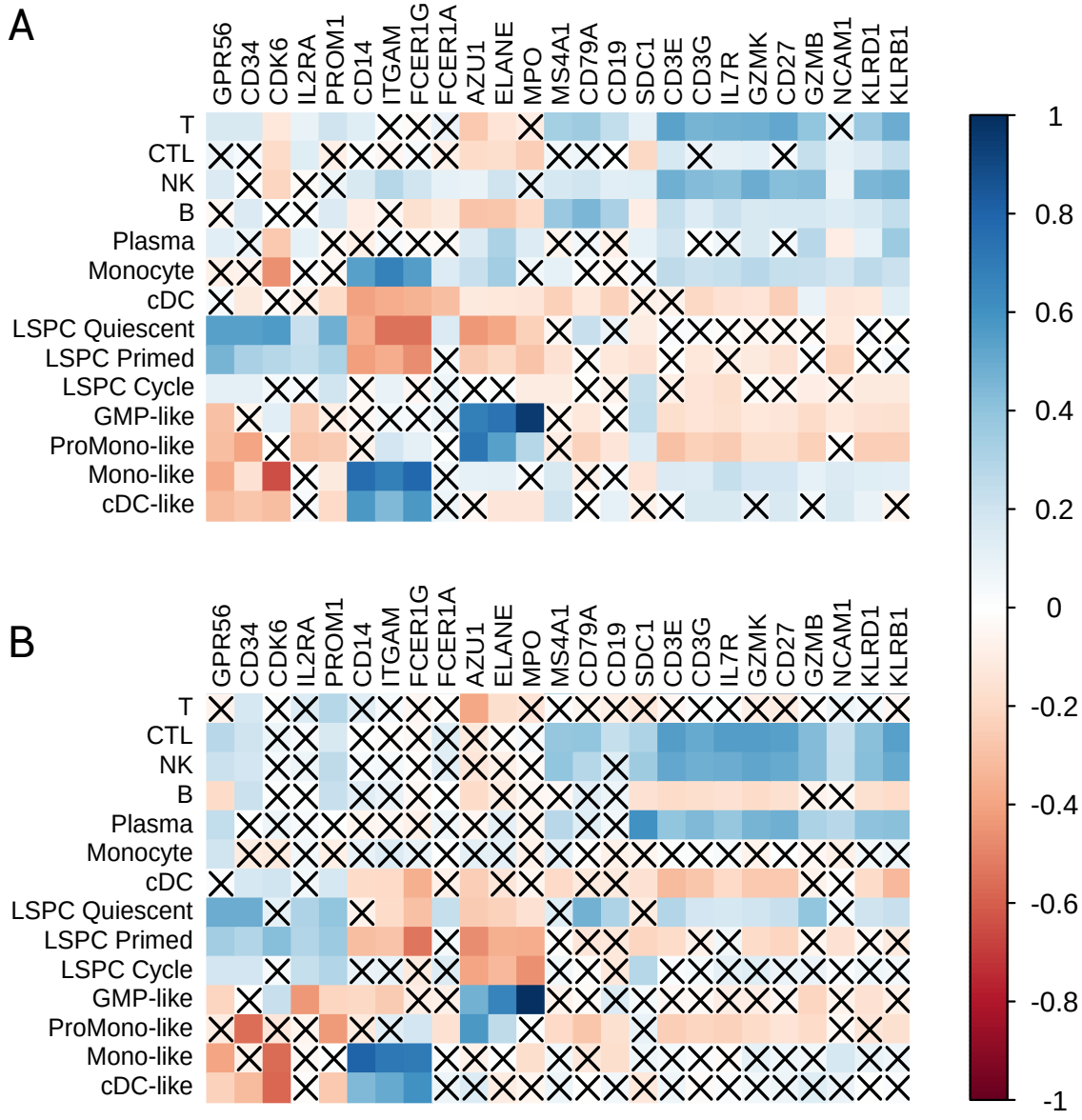

Figure S10. **Correlation matrix plot between lineage-related genes expression and compartmental transcriptional contribution scores.** To the right, a color scale indicates both correlation nature and strength according to a Spearman's rho (ρ). Each element that composes this matrix corresponds to a single correlation analysis. Gene symbols listed in dark blue are for inflammasome genes, while gene symbols in red are for autophagy genes, and the black labeled text is for cell compartments that composes a complex sample. The crossed cells (⊠) in the matrix represent the correlations that did not reach the pre-established statistical level of significance ($p > 0.05$). (A) plot represent BeatAML 1.0 cohort data, and (B), the TCGA AML cohort. The denomination "-like" regard malignant cell compartments that are, to a certain degree, molecularly similar to their non-malignant counterpart albeit still being neoplastic cells. The lineage-defining genes were obtained from P. van Galen (PMID: 30827681) et al. and Triana et al. (PMID: 34811546) works.